THE JOURNAL OF PHYSICAL CHEMISTRY B

ARTICLE

pubs.acs.org/JPCB

Molecular Dynamics Study on Au/Fe_3O_4 Nanocomposites and Their Surface Function toward Amino Acids

Jeffrey Yue, Xuchuan Jiang,* and Aibing Yu

School of Materials Science and Engineering, University of New South Wales, Sydney NSW 2052, Australia

Supporting Information

ABSTRACT: The deposition of gold nanoparticles on the magnetite (Fe_3O_4) surface is demonstrated through a molecular dynamics method. The simulated results show that an intermediate layer composed by such as a surfactant, polymer, or silica plays a key role in the formation of core/shell Fe_3O_4/Au nanostructures. The functional groups of the intermediate layer are crucial factors in depositing gold onto the Fe_3O_4 surface via nonbonding interactions, in which the van der Waals and Columbic forces will determine the strength of interaction toward the gold and iron oxide. Such interactions can affect the stability of the metal-coated nanocomposites and hence the functional properties. The nanocomposite is further investigated on the surface adsorption of amino acids (e.g., cysteine), which may be useful for functional exploration in biomedical applications.

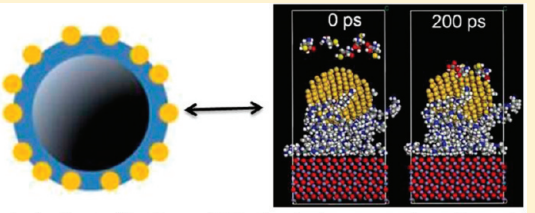

Au/polymer/Fe_3O_4 and MD simulation towards amino acid

1. INTRODUCTION

Metal-coated magnetic nanoparticles have attracted much attention in the past. The combination of two or more materials to form a nanocomposite allows them to exhibit new or enhanced functional properties compared to their individual components.[1] For instance, magnetite (Fe_3O_4) exhibits superparamagnetic properties at the nanoscale, and it has been applied in ferrofluids, magnetic resonance imaging (MRI), and magnetic separation.[2,3] Iron oxide nanoparticles coated with metals (e.g., gold, silver) will enhance its biocompatibility and surface plasmon resonance, which introduces them further to diverse applications such as drug deliveries, plasmonics, and surface-enhanced Raman spectroscopy (SERS).[4−6]

Various techniques have been used to fabricate such nanocomposites, such as deposition using high-energy sources (e.g., ultrasonication, γ-rays, or high-temperature treatment),[7−9] sputter coating under ultrahigh vacuum (UHV) conditions,[10] and the deposition−precipitation method.[11] However, these techniques often produce coatings with wide particle size distribution and may be limited to cluster deposition rather than uniform shell/layer structure. The main difficulty in preparing such particles is due to the weak interaction between iron oxide (e.g., α-Fe_2O_3 and Fe_3O_4) and metal (e.g., Au, Ag, Pt, and Pd) nanoparticles. An alternative solution is to modify the surface of iron oxides with an intermediate layer such as surfactants,[5,12] polymers,[13,14] or an amorphous Si−OH polymerizer.[15] The coated surface can introduce new functional groups such as carboxylates, amines, or thiols, which provide a strong linkage between the iron oxide and the gold nanoparticles (AuNPs).

Despite some successes in experimental synthesis, the role the intermediate layer played in the formation of core/shell structures is not properly understood, and methods to obtain the quantitative information regarding the interaction of molecules of gold and iron oxide surfaces remain a challenging task. This will limit the possibility of materials used to synthesize these nanostructures. To move beyond the physical phenomena, a theoretical simulation method will be beneficial to predict the stability and functionality of nanocomposites, particularly for the synthesis of stable particles during its in vivo application and its removal after use.[16]

In this study, the molecular dynamics (MD) method is used to simulate the interaction of AuNPs depositing onto the modified Fe_3O_4(111) surface. Molecules with various functional groups are investigated in this study, including: oleylamine (OM), oleic acid (OA), polyethylimine (PEI), polymethylacrylic acid (PMAA), 3-aminopropyl triethylsilane (APTES), and tetraethylorthosilicate (TEOS). The surface adsorption of amino acid molecules, cysteine, methionine, and arginine, onto Au/PEI/Fe_3O_4 is simulated to understand the possibility of magnetic separation applications. These results will be useful for understanding the bonding mechanisms of the intermediate layer in the core/shell nanostructures at a molecular scale.

2. NUMERICAL METHOD

Various theoretical methods such as density functional theory and Monte Carlo simulations have been used to simulate the Fe_3O_4 surface.[17,18] In this study, the MD method is used due to its efficiency and capacity to perform simulations at the nanoscale and to track the atomic motion of macromolecules and nanoclusters.[19,20] The simulation was performed at 298 K with a canonical ensemble (NVT) using the Discover module of Material Studio (version 4.4, Accelrys Inc., 2007). The COMPASS

Received: July 11, 2011
Revised: August 30, 2011
Published: September 06, 2011

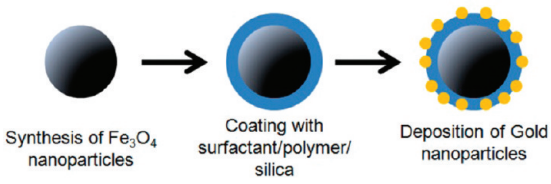

Figure 1. Scheme of the synthesis procedure of layer-by-layer coating into Fe_3O_4/Au core/shell nanostructures.

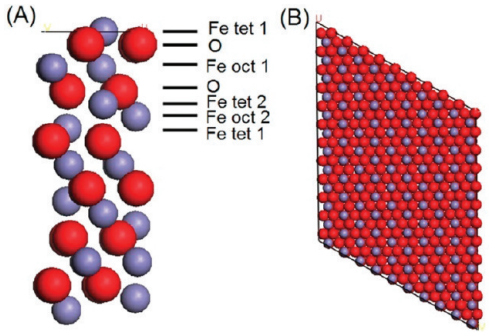

Figure 2. Atomic arrangement of the $Fe_3O_4(111)$ surface used in calculation. (A) Side view showing the termination of the Fe_{tet1} atom and (B) top view of the surface in the expanded supercell.

(Condensed-phase Optimized Molecular Potentials for Atomistic Simulation Studies) force field (see Supporting Information) is used to calculate the potential energy of the systems, in which the parameters derived from ab initio can be applied to predict gas-phase and condensed-phase properties of organic and inorganic materials.[21,22]

To understand the mechanism of the AuNPs depositing onto the modified $Fe_3O_4(111)$ surface, two separate steps are simulated, as illustrated in Figure 1. The Fe_3O_4 particles are first coated using a surfactant, polymer, or silica-based material, followed by depositing the AuNPs onto the modified Fe_3O_4 surface. In our model, the crystal cell consists of a AuNP with size ~1.5 nm (250 atoms); a surface coating with ~1000 atoms (12 repeating units for polymers such as PEI and PMAA); and the $Fe_3O_4(111)$ surface (dimension: thickness T = 15 Å, u = 29.6 Å, v = 35.6 Å, and γ = 120°). The $Fe_3O_4(111)$ surface is cleaved according to the studies obtained from surface and ab initio simulations with Fe_{tet1} terminations as shown in Figure 2.[17,23,24] This surface is particularly chosen because of its stability compared with other crystal planes under the oxygenated atmosphere and the adsorption of molecules.

The molecules used as an intermediate layer to coat the $Fe_3O_4(111)$ surface are chosen according to previous reports, which includes OM,[25] PEI,[26,27] and APTMS/APTES.[28,29] As a comparison, OA,[30] PMAA,[31] and TEOS[32] are also used as case studies to compare the effectiveness for the bonding of magnetite and gold surfaces. The molecular structures of these molecules are shown in Figure 3. The simulation of the coating layer is run for 100 ps with the time step of 1 fs. The AuNP is then placed over the modified surface and further continued for another 300 ps.

To test the possible application for magnetic separation of biomolecular species, the adsorption of amino acid molecules, cysteine (Cys), methione (Met), and arginine (Arg), was tested. The model consists of the addition of five amino acid molecules

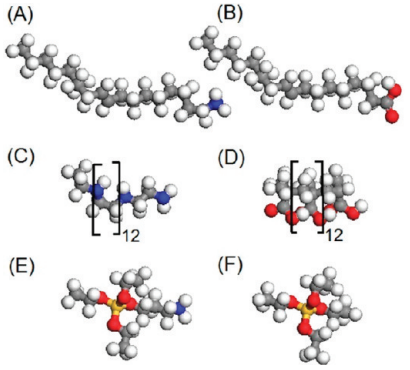

Figure 3. Molecular structure of the molecules used in simulation: (A) oleylamine (OM), (B) oleic Acid (OA), (C) polyethyleimine (PEI), (D) polymethylacrylic acid (PMAA), (E) 3-aminopropyl triethylsilane (APTES), and (F) tetraethylorthosilicate (TEOS).

placed randomly at a distance from the surface, and the simulation is further continued for another 200 ps.

The interaction energy between the AuNP and the iron oxide surface is calculated by the equation

$$E_{\text{interaction}} = E_{\text{total}} - (E_{\text{surface}} + E_{\text{nanoparticle}}) \quad (1)$$

The energy of a system can be expressed as a sum of the bonded and nonbonded interactions

$$E_{\text{total}} = E_{\text{bonded}} + E_{\text{nonbonded}} \quad (2)$$

The energy of bonded interactions includes: bond stretching (bond), valence angle bending (angle), dihedral angle torsion (torsion), and out-of-plane interactions (oop)

$$E_{\text{bonded}} = E_{\text{bond}} + E_{\text{angle}} + E_{\text{torsion}} + E_{\text{oop}} \quad (3)$$

The interaction energies between nonbonded atoms account for: van der Waals (vdW), electrostatic (Coulomb), and hydrogen bond (hbond)

$$E_{\text{nonbond}} = E_{\text{vdW}} + E_{\text{Coulomb}} + E_{\text{hbond}} \quad (4)$$

3. RESULTS AND DISCUSSION

3.1. Molecular Interactions with the $Fe_3O_4(111)$ Surface. The successful coating of molecules onto iron oxides is highly dependent on the interaction of the functional groups. The molecular layer plays a key role by bonding simultaneously with both the iron oxide surface and the AuNPs. Thus, we selected molecules that have been frequently used in the synthesis of Fe_3O_4/Au core/shell nanoparticles for shape and size control. To understand the structural characteristics of the intermediate layer, we will first analyze the interaction energies between the molecules and the $Fe_3O_4(111)$ surface.

During the MD simulation, the molecules move closely toward the surface and adsorb onto stable sites of the Fe_3O_4-(111) surface. The model used in this case contains a thick coating to represent a fully coated layer of molecules on the magnetite surface. It is observed that the molecules could adsorb to form a relatively smooth surface rather than aggregating into clusters. This means that the molecule−metal oxide interactions are favored over the molecule−molecule interactions. By calculating the interaction of these molecules on the $Fe_3O_4(111)$ surface, the stability of the molecules in the formation of a coating

Table 1. van der Waals and Electrostatic Interaction Energies (kcal/mol) of the Molecules on the $Fe_3O_4(111)$ Surface After 100 ps and the AuNP on the Modified $Fe_3O_4(111)$ Surface after 300 ps

	coating on $Fe_3O_4(111)$		gold deposition	
	van der Waals	electrostatic	van der Waals	electrostatic
unmodified Fe_3O_4 surface	–	–	−148.1	0.0
oleylamine	−160.4	−110.7	−708.0	0.0
oleic acid	−156.9	−52.7	−425.2	0.0
PEI	−152.6	−773.5	−408.7	0.0
PMAA	−96.5	−618.3	−288.1	0.0
APTES ($-C_3H_6NH_2$ silica)	−174.1 (−181.2)	−612.5 (−577.7)	−445.9	0.0
TEOS (−OH silica)	−184.4 (−179.5)	−460.4 (−568.7)	−150.6	0.0

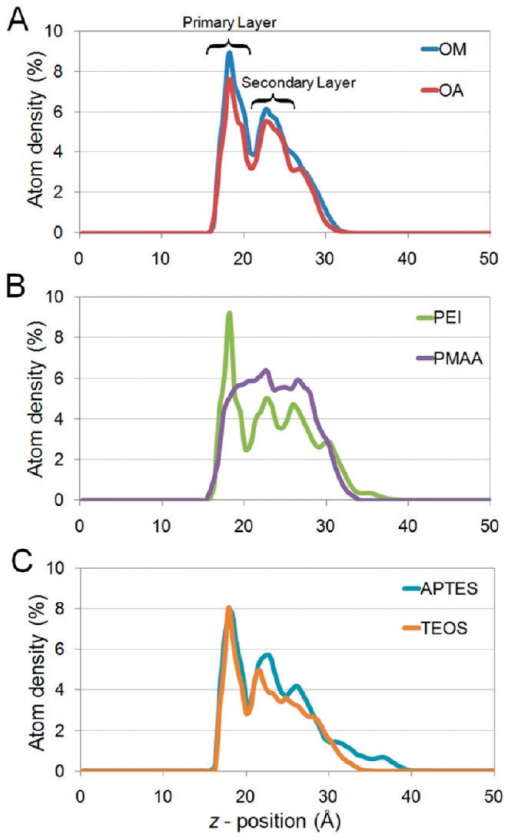

Figure 4. Concentration profile of the (A) surfactant, (B) polymer, and (C) silane molecules on the $Fe_3O_4(111)$ surface along the *z*-direction.

layer can be estimated. The comparison of the interactions of these molecules on the $Fe_3O_4(111)$ surface is shown in Table 1. The data reveal that the van der Waals interactions remain relatively constant in each system, while the electrostatic interaction varies depending on the functional group(s) in the molecule. Generally, the polymers have much higher interaction energy than the surfactant molecules because more functional groups are available for interaction, and the amine group has a stronger attractive force than the carboxyl groups.

The structural configuration of the molecules on the surface is compared by using the concentration profile as plotted in Figure 4. The curvature of the graph shows a high concentration of atoms close to the lattice surface forming the first layer or the "primary layer", in which the molecules are closely bound toward the $Fe_3O_4(111)$ lattice atoms. The smaller peaks indicate the formation of a "secondary layer", where the atoms further away from the surface are highly movable. The only exception in these cases is the PMAA molecules under the reported conditions. The polymer chains with highly branched functional groups tend to entangle with neighboring molecules rather than closely toward the $Fe_3O_4(111)$ surface.

The formation of the separate layers on a surface is consistent with the previous experimental and simulation studies.[33,34] Henderson et al.[35] reported that the PDMS polymer melt on the silica surfaces region does not represent the bulk polymer since it is a part of the bound layer. The orientated polymer chains will appear with elongated and flattened configuration close to the particle surface, hence strong atomic density is close to the surface. This can be confirmed by the glass transition analysis of such polymer film structures, which shows two peaks indicating the bulk (loose packing) and surface (tight binding) properties of the polymers.[36,37] The stability of this coating layer will be crucial in the deposition of the AuNPs. Surfactant molecules are often used as shape control agents for iron oxides in hydrothermal reactions because they can coat on the surface to form a thin film with self-assembled structure.[38,39] Moreover, the strong attraction of the polymers and silanes is in good agreement with previous studies, where the functional groups can interact with the metal oxide surface when the nanocomposite is formed.[27,28]

Here, the APTMS and TEOS molecules are assumed to polymerize into a 3D amorphous structure on the oxide surfaces in the experimental synthesis; however, it is a complicated system if considering the whole network in MD simulation. Theoretically, the function groups of $-C_3H_6NH_2$ in APTMS and −OH in amorphous silica are considered as surface terminations but not the whole polymerized network. The functional groups play a key role in the surface coating on iron oxide as well as bonding with AuNPs. From our MD simulations, the interaction energies are similar for monomer silane(s) and polymerized amorphous silica, which indicates that the structure of either monomer molecules or polymerization is still comparable.

3.2. Interaction of Gold with the Modified $Fe_3O_4(111)$ Surface. The simulation with the addition of the AuNP is continued for another 300 ps, as shown in Figure 5. The snapshots of the simulation show that the nanoparticle moves slowly toward the surface of $Fe_3O_4(111)$, while the surfactant or polymer layer gradually moves toward the AuNP and surrounds it. In comparison, the silica layer can only vibrate rather than surround the AuNP due to its inflexible 3D network structure after polymerization. The comparison of the interaction energies

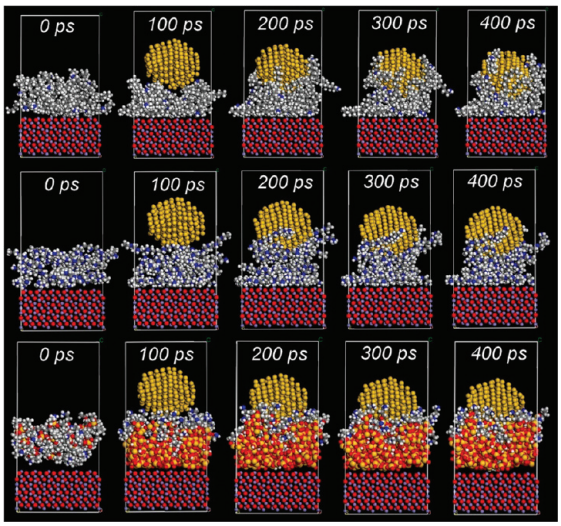

Figure 5. Snapshots of (top) OM, (middle) PEI, and (bottom) APTES-silica coating onto the surface of $Fe_3O_4(111)$ and the addition of a AuNP at various times.

of gold onto the modified surface (Table 1) clearly indicates that a modified surface can change the interaction of the deposited gold cluster. On the basis of the interaction energies, we also realized that the interaction with gold is significantly dependent on the van der Waals forces rather than on electrostatic force.

The simulation of the surfactants, OM and OA, shows interaction energies of −708.0 and −425.2 kcal/mol, respectively. They are stronger than the interaction with an unmodified surface, −148.1 kcal/mol. The reason can be explained by the ability of the surfactant molecules to move and encapsulate the surface of the AuNPs and stabilize the overall structure. Although OM and OA are similar in molecular structure, the charge polarity of the functional group is slightly different in bonding gold atoms.[40] The stronger charge of the amine group in OM can therefore interact strongly with the Au and Fe_3O_4 surfaces.[41,42] The significantly stronger interaction between OM−AuNP than that between OA−AuNP could be due to the coordination interaction between Au and N atoms. The CH chain is similar in OM and OA, so it has a similar contribution to the interaction. Therefore, the difference probably comes from the interaction between Au−N and Au−O because N in NH_2 could have a stronger coordination with the Au atom than OH with the Au atom. This may be also useful for understanding the difference in interactions between PEI or PMAA and AuNPs.

Similar movements are observed during the simulation of PEI (middle, Figure 5). In the first 100 ps, the chains of polymer molecules are attracted to the magnetite surface, and the addition of the AuNP will also move toward the modified surface with an interaction energy of −408.7 kcal/mol. The slightly lower interaction is due to the strong interaction of PEI onto the $Fe_3O_4(111)$ surface rather than with the AuNP. Nevertheless, the interaction is enhanced by the (semi)encapsulation of PEI molecules toward the AuNP. The mechanism for such enhancement can be further understood by comparing PEI with PMAA in the following context.

Although PMAA/iron oxide nanocomposites can be commonly prepared, it is still a challenge to deposit AuNPs onto a PMAA-modified iron oxide surface.[43,44] Its interaction energy is calculated to be −288.1 kcal/mol, which is relatively weaker than that of PEI under similar conditions. Theoretically, the carboxyl group of PMAA can interact strongly with smooth surfaces of Fe_3O_4 and gold.[45] However, as an intermediate layer for interacting with spherical AuNPs, it involves the rotation and bending of the polymer molecule to encapsulate the structure. The problem for the PMAA molecule is that it cannot reorganize its structure because the branching of the $-CH_3$ and $-CH_2COOH$ groups does not allow such physical reorientation, whereas the highly linear molecules such as PEI can freely bend and rotate their carbon chains to wrap the AuNP. Moreover, the branching of the functional groups in the molecule causes aggregation and entangled chains on the $Fe_3O_4(111)$ surface, as shown in the concentration profile in Figure 4. The polymer coating without a "soft" (secondary and third) layer will reduce the mobility of the molecule and hence increase the difficulty to move toward the AuNP.

On the contrary, the surface of polymerized silica differs from other surfactants and polymers used in the MD simulation. The SiO_2 structure is bonded as a 3D network rather than as a 1D chain structure, which may limit the mobility of silica on the surface of iron oxide. To be consistent with the previous study that the amorphous silica can be terminated with silanols (Si−OH), silanethyl ($Si-(CH_2)_xH$), or amine ($Si-(CH_2)_xNH_2$) groups according to the solvents used,[46] our simulation model consists of a surface terminated with $-(CH_2)_3-NH_2$ and −OH groups. This model is also a good representation of the surface under water-based solution conditions. The structure of silica can be broken with the use of concentrated NaOH.[47] The aim of this study is to compare various interfaces with and without the amine $-NH_2$ functional group during the deposition of gold nanoparticles.

The calculated interaction energy of this Au−SiO_2 or Si−OH system also produces a strong attraction with the AuNPs at −445.9 kcal/mol. In addition, the amino group can strongly interact with the Au atoms, but the propyl chain plays a key role in encapsulating the nanoparticles. Fang et al.[48] reported the use of TEOS to coat α-Fe_2O_3 nanospheres followed by a second-layer coating with ATPMS. They mentioned that it is necessary to functionalize the surface with amino groups to produce the α-Fe_2O_3@SiO_2@Au nanocomposites. This is because the aminopropyl group exposed on the surface can interact with other molecules and/or particles.[49,50] Ge et al.[51] also found that the 3-(methacryloyloxy)propyl functional group could produce similar nanocomposites. Therefore, the termination of silica coatings with long alkyl groups can benefit from a higher physical interaction with the AuNPs by wrapping the particle surface.

As a referencing material, we performed the simulation of gold depositing onto a silanol terminated (Si−OH) silica surface.[52] This model represents a nonfunctionalized surface produced under water solution conditions. The interaction energy between gold and the silanol surface is estimated at −150.6 kcal/mol, which is similar to the case with an unmodified Fe_3O_4 surface. This is probably caused by the network structure of SiO_2 and the Si−OH group, which does not allow significant surface atomic motion or exhibit the relevant functional groups.[53]

3.3. Role of the Intermediate Layer. By comparison with the interaction energies of different materials coated on the Fe_3O_4-(111) surface, it is found that the mobility of the surface molecules plays a key role in improving the interaction with the deposited AuNP. The surface molecules can form secondary (and third) layer(s), which weakly interact with the iron oxide surface, and thus the surface coating can move toward the AuNP

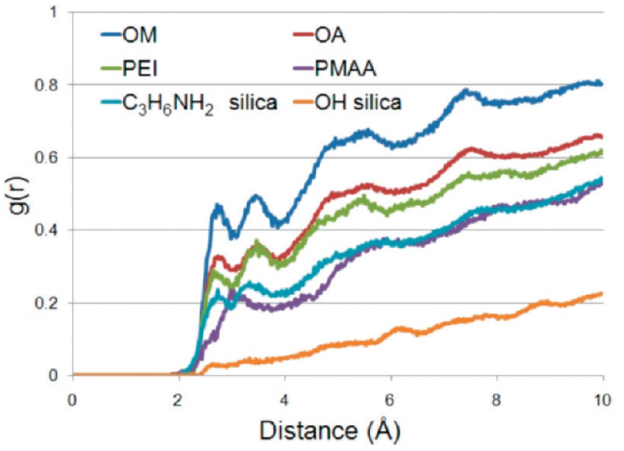

Figure 6. Radial distribution functions of various coatings with Au atoms.

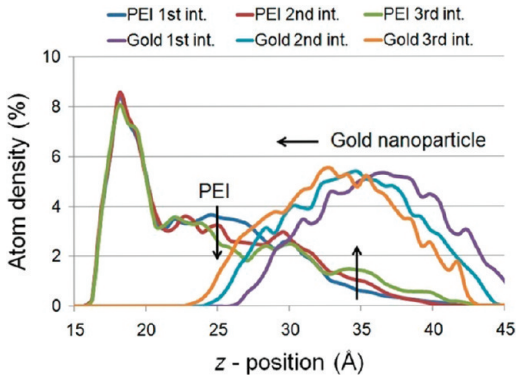

Figure 7. Concentration profile of the molecules on the $Fe_3O_4(111)$ surface along the (001) direction. The first, second, and third interval represents time between 1 and 100, 101 and 200, and 201 and 300 ps, respectively.

and stabilize the structure. This can be further illustrated through the radial distribution function curves in Figure 6, in which the interaction energies correlate to the amount of atoms coated onto the Au surface. The higher intensity for OM, OA, PEI, and $C_3H_6NH_2$ silica indicates that the molecules are in close contact with the Au surface, whereas PMAA and OH silica cannot move toward the surface due to structural limitations.

This can be further confirmed by the atomic concentration profile of the Au/PEI/Fe_3O_4 system at different simulation times (Figure 7). The AuNP moves toward the PEI-modified surface throughout the simulated time steps; at the same time, the molecular chain of PEI also changes in the presence of gold such that the molecules in the secondary layer will move toward the AuNP. This results in PEI molecules creeping along the nanoparticle surface, hence decreasing atomic concentration in the 22−27 Å region and moving toward the 32−41 Å region. However, no changes are observed to the primary layer throughout the simulation, which indicates the adsorbed layer is highly stable on the primary layer, while the secondary (and third) layer(s) can move to other surfaces/particles. Hence, the stability of the overall nanocomposite depends on the intermolecular bond strength. This means that smaller molecules are less favorable in the preparation of metal-coated structures, whereby the use of large molecules or network structures such as polymers and silica is much more favorable. Here we need to point out that the molecular weight (MW) of polyethylimine is relevant to the chain length of polymer, which may affect the formation of layer(s) of PEI on the Fe_3O_4 surface as well as on AuNPs, confirmed by the above simulation results.

Moreover, the bonding strength of these structures is highly dependent on the positive amine groups attracting to the metal nanoparticles, which are rich in electrons along the surface.[26,54] The positive charge of NH_2 group(s) in OM, PEI, and APTES can attract on the highly oxygenated sites of Fe_3O_4. The electrostatic interaction is extensively increased for PEI from the number of nitrogen atoms, whereas the low interaction of OM only has one functional group with a nonpolar carbon chain. On the contrary, it is also possible for negative-charged carboxyl groups of OA and PMAA to find interactive sites on the Fe_{tet1} terminated $Fe_3O_4(111)$ surface based on our simulation findings. However, the long-chain molecular structure is also important as an intermediate layer, which forms a stable coating on the Fe_3O_4 surface, thus the "soft" molecular layers can encapsulate the deposited AuNP readily. Note that in the present MD simulation the gold atoms are presumed as a neutral surface, and the surface charge on AuNPs is proposed to originate from the coated surfactant molecules with different functional groups like $-NH_2$ and $-OH$, although the gold atoms or clusters obtained in experiments are a negative surface due to a charge distribution on the surface. However, the fundamental understanding of negative gold atoms is beyond the MD simulation. Future work using the density functional theory method will be conducted to investigate this issue.

3.4. Surface Function of the Au/Fe_3O_4 Nanocomposite. The advantages of metal-coated iron oxide nanocomposites can be demonstrated as a few aspects, such as reducing aggregation of particles, maintaining the magnetic stability, slowing down the degrading process under physiological conditions, and reducing toxicity.[55] So far, they have shown promising applications for monitoring inside living cells by magnetic resonance (MR)/fluorescence imaging, magnetic separations, and drug delivery vehicles.[56] The nanocomposites are highly superior to single particles, in which they may extend the adsorbed chemical species and avoid time-consuming techniques used in the filtration or centrifugation process.[57]

To understand the adsorption behavior of amino acids/proteins onto magnetic nanoparticles, the interaction of the amino acids, cysteine (Cys), methionine (Met), and arginine (Arg), is tested on the Au/PEI/Fe_3O_4 surface. Figure 8A−C shows the molecular structures of these molecules, and Figure 8D shows the addition of cysteine molecules and its adsorption onto the Au-deposited structure after 200 ps. It is observed that the molecules will gradually approach the AuNP, and some molecules will adsorb quickly. The motion of the molecules can be tracked by the mean squared displacement (MSD) of the amino acid molecules (Figure 9A). It is found that cysteine strongly interacts with Au atoms due to the high affinity of the S−Au bond, which is consistent with the previous studies related to thiol−gold bonding. The reason for a stronger attraction can be observed in the radial distribution function curve of the functional groups with the Au atoms (Figure 9B). The data show that the S−H functional group is highly orientated toward the Au atoms at a discrete position, while the C−S−C, N−H, and OH tend to vibrate on the surface. This reveals that the nanocomposite material is selective toward the functional groups present in the molecules.

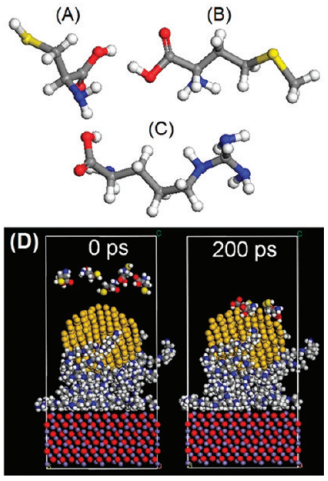

Figure 8. Molecular structure of (A) cysteine, (B) methinone, and (C) arginine and (D) snapshots of the Au/PEI/Fe_3O_4 nanocomposite with the addition of cysteine at simulation time of 0 and 200 ps.

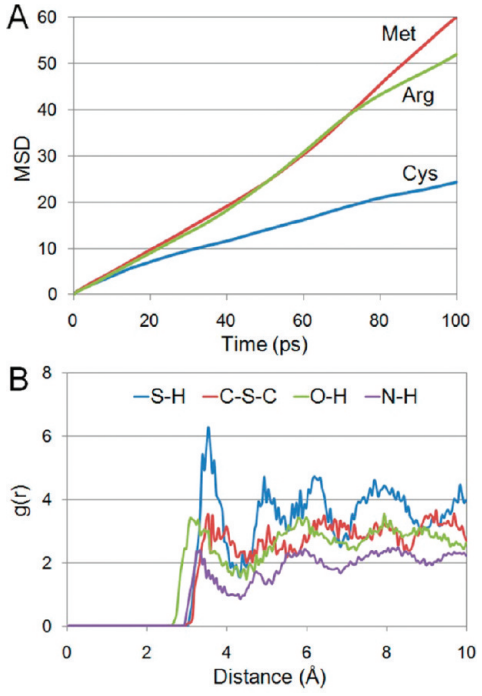

Figure 9. (A) Mean squared displacement (MSD) of the amino acid molecules on the Au/PEI/Fe_3O_4 surface and (B) the radial distribution function of various functional groups with Au atoms.

Although the gold has a strong interaction with amino acids, the Au/PEI/Fe_3O_4 has been considered as a whole structure, in which the role of iron oxide substrate (magnetite slab) is not only used for supporting the gold particles for more applications[55−57] but also used in the simulation to account for the attractive and repulsive forces that may affect the final interaction energies due to the interaction mediated by PEI molecules. Similarly, Kinoshita et al.[58] demonstrated that the sulfur containing amino acids, namely, cysteine and methionine, can absorb onto Au/γ-Fe_2O_3 composites. The results show that the cysteine molecules can be fully separated using the Au/γ-Fe_2O_3 (Au 44 wt %) and show 50% efficiency for methionine molecules. However, bare γ-Fe_2O_3 particles have an insignificant adsorption on all amino acids, which indicates the importance of AuNP during selective adsorption of molecules. In addition, Sun et al.[59] used the density functional theory method for simulation in a similar system. The calculation also shows that cysteine has a stronger interaction than methionine, with binding energies of 0.738 and 0.712 eV, respectively. It is suggested that the 3p energy level in the sulfur atom is significantly close to the 6s orbital in gold, which makes the Au−S bonding more favorable compared with others (B, C, N, O, and Si). This phenomenon therefore suggests that the higher oxidation state of sulfur (e.g., sulfates) cannot form stable bonds with gold. However, we need to point out that it is still difficult to fully understand the interaction between various functional groups and the AuNP using the MD method because the atomic electron densities have not been considered, which is beyond the capacity of the current MD simulation. Nonetheless, the applied MD simulation method can help estimate the interaction energies of molecular scale and predict the molecular motions on the gold surface.

4. CONCLUSIONS

This study has demonstrated the role of the intermediate layer during the deposition of AuNPs onto the Fe_3O_4(111) surface using the MD method. It was found that the interaction between AuNPs and the Fe_3O_4(111) surface can be enhanced by modifying the Fe_3O_4 surface using suitable surfactants, polymers, and Si−OH terminated amorphous polymer. The strength of the interaction toward the Fe_3O_4 surface is dependent on the functional groups available in the molecule for electrostatic interactions. For intermediate molecules, the amine functionalized molecules such as OM, PEI, and APTES can interact with the Fe_3O_4 surface to form a strongly bonded "primary layer", but loosely packed molecules are formed in a "secondary layer", which is critical for encapsulating the AuNPs to increase the van der Waals interaction. Considering the interaction of amino acids with Au/PEI/Fe_3O_4 nanocomposites, cysteine has a relatively strong absorption. The strong sulfur−gold bond can reduce the diffusivity of the molecule to form a stable attachment on the Au-coated structure. The iron oxide substrate may affect the interaction forces during MD simulation. The results will be useful for understanding the interaction of the metal deposited metal oxide nanocomposite and for determination of possible surface sensing applications.

■ ASSOCIATED CONTENT

Supporting Information. Table of list of force fields (COMPASS) used in the present MD simulation. This material is available free of charge via the Internet at http://pubs.acs.org.

■ AUTHOR INFORMATION

Corresponding Author

*E-mail: xcjiang@unsw.edu.au.

■ ACKNOWLEDGMENT

We gratefully acknowledge the financial support of the Australian Research Council (ARC) through ARC Discovery Projects. The authors acknowledge access to the University of New South Wales (UNSW) node of the Australian Microscopy & Microanalysis Research Facility (AMMRF).

REFERENCES

(1) Xiao, Y.; Li, C. M. *Electroanalysis* **2008**, *20*, 648.
(2) Erogbogbo, F.; Yong, K. T.; Hu, R.; Law, W. C.; Ding, H.; Chang, C. W.; Prasad, P. N.; Swihart, M. T. *ACS Nano* **2010**, *4*, 5131.
(3) Casula, M. F.; Floris, P.; Innocenti, C.; Lascialfari, A.; Marinone, M.; Corti, M.; Sperling, R. A.; Parak, W. J.; Sangregorio, C. *Chem. Mater.* **2010**, *22*, 1739.
(4) Larson, T. A.; Bankson, J.; Aaron, J.; Sokolov, K. *Nanotechnology* **2007**, *18*, 325101.
(5) Wang, L.; Park, H. Y.; Lim, S. I. I.; Schadt, M. J.; Mott, D.; Luo, J.; Wang, X.; Zhong, C. J. *J. Mater. Chem.* **2008**, *18*, 2629.
(6) Arsianti, M.; Lim, M.; Lou, S. N.; Goon, I. Y.; Marquis, C. P.; Amal, R. *J. Colloid Interface Sci.* **2011**, *354*, 536.
(7) Seino, S.; Kinoshita, T.; Otome, Y.; Maki, T.; Nakagawa, T.; Okitsu, K.; Mizukoshi, Y.; Nakayama, T.; Sekino, T.; Niihara, K.; Yamamoto, T. A. *Scr. Mater.* **2004**, *51*, 467.
(8) Pradhan, A.; Jones, R. C.; Caruntu, D.; O'Connor, C. J.; Tarr, M. A. *Ultrason. Sonochem.* **2008**, *15*, 891.
(9) Jiang, X. C.; Yu, A. B. *J. Mater. Process. Technol.* **2009**, *209*, 4558.
(10) Sun, Y. N.; Qin, Z. H.; Lewandowski, M.; Shaikhutdinov, S.; Freund, H. J. *Surf. Sci.* **2009**, *603*, 3099.
(11) Liu, X.; Zhang, J.; Guo, X.; Wu, S.; Wang, S. *Nanotechnology* **2010**, *21*, 095501.
(12) Park, H. Y.; Schadt, M. J.; Wang, L.; Lim, I.-I. S.; Njoki, P. N.; Kim, S. H.; Jang, M. Y.; Luo, J.; Zhong, C. J. *Langmuir* **2007**, *23*, 9050.
(13) Zhai, Y.; Zhai, J.; Wang, Y.; Guo, S.; Ren, W.; Dong, S. *J. Phys. Chem. C* **2009**, *113*, 7009.
(14) Spuch-Calvar, M.; Pérez-Juste, J.; Liz-Marzán, L. M. *J. Colloid Interface Sci.* **2007**, *310*, 297.
(15) Caruntu, D.; Cushing, B. L.; Caruntu, G.; O'Connor, C. J. *Chem. Mater.* **2005**, *17*, 3398.
(16) Gupta, A. K.; Gupta, M. *Biomaterials* **2005**, *26*, 3995.
(17) Shimizu, T. K.; Jung, J.; Kato, H. S.; Kim, Y.; Kawai, M. *Phys. Rev. B: Condens. Matter* **2010**, *81*, 235429.
(18) Mazo-Zuluaga, J.; Restrepo, J.; Mejia-Lopez, J. *J. Appl. Phys.* **2008**, *103*, 113906.
(19) Praprotnik, M.; Site, L. D.; Kremer, K. *Annu. Rev. Phys. Chem.* **2008**, *59*, 545.
(20) Sherwood, P.; Brooks, B. R.; Sansom, M. S. P. *Curr. Opin. Struct. Biol.* **2008**, *18*, 630.
(21) Sun, H. *J. Phys. Chem. B* **1998**, *102*, 7338.
(22) Sun, H.; Ren, P.; Fried, J. R. *Comput. Theor. Polym. Sci.* **1998**, *8*, 229.
(23) Yang, T.; Wen, X. D.; Ren, J.; Li, Y. W.; Wang, J. G.; Huo, C. F. *J. Fuel Chem. Technol.* **2010**, *38*, 121.
(24) Lemire, C.; Meyer, R.; Henrich, V. E.; Shaikhutdinov, S.; Freund, H. J. *Surf. Sci.* **2004**, *572*, 103.
(25) Xu, Z.; Hou, Y.; Sun, S. *J. Am. Chem. Soc.* **2007**, *129*, 8698.
(26) Goon, I. Y.; Lai, L. M. H.; Lim, M.; Munroe, P.; Gooding, J. J.; Amal, R. *Chem. Mater.* **2009**, *21*, 673.
(27) Xie, H. Y.; Zhen, R.; Wang, B.; Feng, Y. J.; Chen, P.; Hao, J. *J. Phys. Chem. C* **2010**, *114*, 4825.
(28) Spuch-Calvar, M.; Pacifico, J.; Pérez-Juste, J.; Liz-Marzán, L. M. *Langmuir* **2008**, *24*, 9675.
(29) Wang, H.; Brandl, D. W.; Le, F.; Nordlander, P.; Halas, N. J. *Nano Lett.* **2006**, *6*, 827.
(30) Pal, S.; Morales, M.; Mukherjee, P.; Srikanth, H. *J. Appl. Phys.* **2009**, *105*, 07B504.
(31) Chibowski, S.; Patkowski, J.; Grzadka, E. *J. Colloid Interface Sci.* **2009**, *329*, 1.
(32) Zhang, Y.; Xu, S.; Luo, Y.; Pan, S.; Ding, H.; Li, G. *J. Mater. Chem.* **2011**, *21*, 3664.
(33) Starr, F. W.; Schrøder, T. B.; Glotzer, S. C. *Macromolecules* **2002**, *35*, 4481.
(34) Bershtein, V. A.; Gun'ko, V. M.; Egorova, L. M.; Guzenko, N. V.; Pakhlov, E. M.; Ryzhov, V. A.; Zarko, V. I. *Langmuir* **2010**, *26*, 10968.
(35) Henderson, D.; Trokhymchuk, A.; Kalyuzhnyi, Y. V.; Gee, R. H.; Lacevic, N. *J. Phys. Chem. C* **2007**, *111*, 15625.
(36) Chen, L.; Zheng, K.; Tian, X.; Hu, K.; Wang, R.; Liu, C.; Li, Y.; Cui, P. *Macromolecules* **2009**, *43*, 1076.
(37) Robertson, C. G.; Rackaitis, M. *Macromolecules* **2011**, *44*, 1177.
(38) Yue, J.; Jiang, X.; Zeng, Q.; Yu, A. B. *Solid State Sci.* **2010**, *12*, 1152.
(39) Yue, J.; Jiang, X. C.; Yu, A. B. *Solid State Sci.* **2010**, *13*, 263.
(40) Shevchenko, E. V.; Bodnarchuk, M. I.; Kovalenko, M. V.; Talapin, D. V.; Smith, R. K.; Aloni, S.; Heiss, W.; Alivisatos, A. P. *Adv. Mater.* **2008**, *20*, 4323.
(41) Laurent, S.; Forge, D.; Port, M.; Roch, A.; Robic, C.; Vander Elst, L.; Muller, R. N. *Chem. Rev.* **2008**, *108*, 2064.
(42) Quek, S. Y.; Venkataraman, L.; Choi, H. J.; Louie, S. G.; Hybertsen, M. S.; Neaton, J. B. *Nano Lett.* **2007**, *7*, 3477.
(43) Long, Y.; Chen, N. X. *Surf. Sci.* **2008**, *602*, 46.
(44) Yang, X.; Chen, L.; Han, B.; Yang, X.; Duan, H. *Polymer* **2010**, *51*, 2533.
(45) Kozlovskaya, V.; Kharlampieva, E.; Khanal, B. P.; Manna, P.; Zubarev, E. R.; Tsukruk, V. V. *Chem. Mater.* **2008**, *20*, 7474.
(46) Tielens, F.; Gervais, C.; Lambert, J. F. o.; Mauri, F.; Costa, D. *Chem. Mater.* **2008**, *20*, 3336.
(47) Piao, Y.; Kim, J.; Na, H. B.; Kim, D.; Baek, J. S.; Ko, M. K.; Lee, J. H.; Shokouhimehr, M.; Hyeon, T. *Nat. Mater.* **2008**, *7*, 242.
(48) Fang, C.-L.; Qian, K.; Zhu, J.; Wang, S.; Lv, X.; Yu, S.-H. *Nanotechnology* **2008**, *19*, 125601.
(49) Mohapatra, S.; Pramanik, N.; Mukherjee, S.; Ghosh, S.; Pramanik, P. *J. Mater. Sci.* **2007**, *42*, 7566.
(50) Koh, I.; Wang, X.; Varughese, B.; Isaacs, L.; Ehrman, S. H.; English, D. S. *J. Phys. Chem. B* **2006**, *110*, 1553.
(51) Ge, J.; Huynh, T.; Hu, Y.; Yin, Y. *Nano Lett.* **2008**, *8*, 931.
(52) Costa, D.; Tougerti, A.; Tielens, F.; Gervais, C.; Stievano, L.; Lambert, J. F. *Phys. Chem. Chem. Phys.* **2008**, *10*, 6360.
(53) Lee, J.; Lee, Y.; Youn, J. K.; Na, H. B.; Yu, T.; Kim, H.; Lee, S. M.; Koo, Y. M.; Kwak, J. H.; Park, H. G.; Chang, H. N.; Hwang, M.; Park, J. G.; Kim, J.; Hyeon, T. *Small* **2008**, *4*, 143.
(54) Kretzers, I. K. J.; Parker, R. J.; Olkhov, R. V.; Shaw, A. M. *J. Phys. Chem. C* **2009**, *113*, 5514.
(55) Mahmoudi, M.; Simchi, A.; Milani, A. S.; Stroeve, P. *J. Colloid Interface Sci.* **2009**, *336*, 510.
(56) Liong, M.; Lu, J.; Kovochich, M.; Xia, T.; Ruehm, S. G.; Nel, A. E.; Tamanoi, F.; Zink, J. I. *ACS Nano* **2008**, *2*, 889.
(57) Deng, Y.; Qi, D.; Deng, C.; Zhang, X.; Zhao, D. *J. Am. Chem. Soc.* **2008**, *130*, 28.
(58) Kinoshita, T.; Seino, S.; Mizukoshi, Y.; Otome, Y.; Nakagawa, T.; Okitsu, K.; Yamamoto, T. A. *J. Magn. Magn. Mater.* **2005**, *293*, 106.
(59) Sun, Q.; Reddy; Marquez, M.; Jena, P.; Gonzalez, C.; Wang, Q. *J. Phys. Chem. C* **2007**, *111*, 4159.